Engineering 3 (2017) 55–59

Contents lists available at ScienceDirect

Engineering

journal homepage: www.elsevier.com/locate/eng

Research
Tissue Engineering—Article

Tethering of Gly-Arg-Gly-Asp-Ser-Pro-Lys Peptides on Mg-Doped Hydroxyapatite

Alessandro Pistone [a,*], Daniela Iannazzo [a], Claudia Espro [a], Signorino Galvagno [a], Anna Tampieri [b], Monica Montesi [b], Silvia Panseri [b], Monica Sandri [b]

[a] Department of Engineering, University of Messina, Messina 98166, Italy
[b] Institute of Science and Technology for Ceramics, National Research Council of Italy, Faenza 48018, Italy

ARTICLE INFO

Article history:
Received 14 October 2016
Revised 13 January 2017
Accepted 16 January 2017
Available online 20 February 2017

Keywords:
Mg-doped hydroxyapatite
Mesenchymal stem cells
Chemotactic/haptotactic factors
Bone tissue engineering

ABSTRACT

Stem cell homing, namely the recruitment of mesenchymal stem cells (MSCs) to injured tissues, is highly effective for bone regeneration *in vivo*. In order to explore whether the incorporation of mimetic peptide sequences on magnesium-doped (Mg-doped) hydroxyapatite (HA) may regulate the homing of MSCs, and thus induce cell migration to a specific site, we covalently functionalized MgHA disks with two chemotactic/haptotactic factors: either the fibronectin fragment III_1-C human (FF III_1-C), or the peptide sequence Gly-Arg-Gly-Asp-Ser-Pro-Lys, a fibronectin analog that is able to bind to integrin transmembrane receptors. Preliminary biological evaluation of MSC viability, analyzed by 3-(4,5-dimethylthiazol-2-yl)-2,5-diphenyltetrazolium bromide (MTT) test, suggested that stem cells migrate to the MgHA disks in response to the grafted haptotaxis stimuli.

1. Introduction

In recent decades, important advances have been reached in biomaterial-based development for tissue engineering, in the form of substitutes that are able to restore, maintain, or improve organ function [1]. The increase in life expectancy requires scientific efforts to focus on the natural bone-healing process and associated complications. Due to their unlimited supply, engineered bone tissues represent a potential alternative to the conventional use of bone grafts; in addition, they carry no risk of disease transmission [2,3]. Efforts in bone tissue engineering mainly focus on inducing functional bone regeneration via combined cell therapy and biomaterials, which include ceramics as well as non-degradable and biodegradable polymers with different mechanical properties, degradation rates, and chemical functionalities [4–9]. Synthetic hydroxyapatite (HA) ceramics are widely used for human implant coatings because of their high biocompatibility and osteoconductivity [10–12]. HA is a key mineral component in bone and tooth tissue, and has multiple ionic substitutions in the lattice, including CO_3^{2-}, F^-, Mg^{2+}, and Na^+. These substitutions not only change the space group, morphology, stability, and mechanical properties of the HA structure, but are also important for the biological responses of bone cells. For example, carbonates (CO_3^{2-}) promote the growth of apatite crystals, while magnesium (Mg) enhances bone metabolism by stimulating osteoblast proliferation at an early stage of osteogenesis, as is demonstrated by the observation that Mg depletion leads to bone fragility and bone loss [13]. Apatite and calcium-phosphate implant materials with low levels of Mg (i.e., MgHA), as well as biomimetic materials with co-substitution of Mg and B-type carbonate (i.e., substitution of phosphate), enhance the bioactivity of the HA structure [14]. Nanoscale control over the scaffold architecture of these nano-sized biomaterials allows a greater understanding of cell-type-specific sensitivity to topographical features, thus enabling the inclusion of proteins and growth factors, even when not clinically possible, and leading to complex multi-tissue regeneration [15].

* Corresponding author.
E-mail address: pistone@unime.it

http://dx.doi.org/10.1016/J.ENG.2017.01.007

The stem cell homing approach, which involves the recruitment of mesenchymal stem cells (MSCs) to injured tissues, is gaining interest among the different scaffold-based tissue engineering strategies because it is robust for bone regeneration *in vivo*. Homing factors such as chemokines, selectins, and integrins that are covalently bound or absorbed into the ceramic or polymeric scaffold can, in fact, allow MSCs to participate as osteoprogenitor cells in the bones' regenerative process [16–18]. Fibronectin (FN) (type I, II, or III) is a major glycoprotein in the extracellular matrix (ECM) and a member of the integrin family of cell surface molecules, which are involved in various cellular events such as cell adhesion, growth, migration, and the differentiation of osteoblasts. FN type III has a central cell-binding domain (CCBD) containing the Arg-Gly-Asp (RGD) motif. This particular domain confers cell adhesion [19]. Specific peptide sequences containing the RGD motif are often used to enhance integrin-mediated cell adhesion.

In this publication, we report our preliminary results on the coating of MgHA disks with two chemotactic/haptotactic factors: either the fibronectin fragment III_1-C human (FF III_1-C), or the peptide sequence Gly-Arg-Gly-Asp-Ser-Pro-Lys, an FN analog that is able to bind to integrin transmembrane receptors. The covalent anchoring of these factors by means of the bifunctional spacer (3-aminopropyl)triethoxysilane (APTES) prevents their metabolism and migration from the implant site, and allows strict control over the spatial orientation of the biomolecules. In order to explore whether the incorporation of these mimetic peptide sequences onto MgHA regulates the homing of MSCs, thereby inducing cell migration to a specific site, we performed a preliminary *in vitro* study.

2. Materials and methods

Commercial solvents and reagents were used without further purification. The FF III_1-C and the Gly-Arg-Gly-Asp-Ser-Pro-Lys peptide sequence were obtained from Sigma-Aldrich. MgHA was synthesized following a previously reported procedure [14]. The MgHA powders were shaped into disks (diameter: 8 mm; height: 3 mm; weight: 300 mg per disk) using isostatic pressure at 2.5 × 10^5 kPa and were stored in a vacuum desiccator at room temperature. An X-ray diffraction (XRD) analysis was performed with a Bruker D8 Advance diffractometer using nickel-filtered Cu$K\alpha$ radiation. Diffraction peaks were compared with those in the Joint Committee on Powdered Diffraction Standards (JCPDS) database. Scanning electron microscopy (SEM) was conducted on a FEI Quanta 450 FEG instrument operating at 15 kV. Transmission electron microscopy (TEM) analyses were carried out with a JEOL JEM-2010 transmission electron microscope (LaB_6 electron gun) at 200 kV. A Gatan 794 multi-scan charge-coupled device (CCD) camera was used to obtain digital images. A TA Q500 instrument was used for thermogravimetric analyses (TGAs) from 100 °C to 1000 °C, with a rate of 10 °C per minute under nitrogen. Infrared analysis on KBr-based pellets was performed in a Fourier transform infrared (FTIR) spectrometer (Perkin-Elmer 2000). Ultraviolet (UV) spectra were analyzed with a Thermo Nicolet Evolution 500 spectrophotometer. All of the MgHA functionalization syntheses in double and non-functionalized disks were used as controls.

All cell-handling procedures were performed in a sterile laminar flow hood. Cultured cells were incubated at 37 °C with 5% CO_2.

2.1. Synthesis of MgHA-APTES disks

The synthesis of the MgHA-APTES disks was performed by immersing the MgHA disks in a 1 mol·L^{-1} solution of APTES in dry hexane (50 mL) while stirring for 3 h at room temperature. Samples were washed with hexane and further dried by vacuum at 40 °C under vacuum for 24 h. The amount of APTES that was grafted onto the disks was evaluated by analyzing the concentration of the free amino groups (NH_2) exposed on the disk surfaces (Kaiser test).

2.2. Synthesis of MgHA-APTES-CFF disks

In a manner similar to the functionalization procedure described above, MgHA-APTES disks were treated with solutions of FF III_1-C (10 μmol·L^{-1} or 100 μmol·L^{-1}) in phosphate-buffered solutions (PBSs, 50 μL or 500 μL), activated with 1-ethyl-3-(3-dimethylaminopropyl) carbodiimide hydrochloride (EDC·HCl, 0.0014 μmol or 0.014 μmol) and *N*-hydroxysuccinimide (NHS, 0.0014 μmol or 0.014 μmol) for 3 h at 37 °C. After functionalization, the samples of MgHA-APTES-CFF10 (chemotactic factors: fibronectin) (10 μmol·L^{-1} concentration of FN) and MgHA-APTES-CFF100 (100 μmol·L^{-1} concentration of FN) were washed with PBS for 10 min and further dried by vacuum at 37 °C for 24 h. The quantity of fibronectin bound onto the MgHA-APTES surface was assessed by nuclear magnetic resonance (NMR) spectroscopy.

2.3. Synthesis of MgHA-APTES-CFP disks

The MgHA-APTES disks were allowed to interact with solutions of the Gly-Arg-Gly-Asp-Ser-Pro-Lys peptide sequence (10 μmol·L^{-1} or 100 μmol·L^{-1}) in PBS (50 μL or 500 μL), activated with EDC·HCl (0.0138 μmol or 0.138 μmol) and NHS (0.0138 μmol or 0.138 μmol) for 3 h at 37 °C. After functionalization, the samples of MgHA-APTES-CFP10 (chemotactic factors: peptide) (10 μmol·L^{-1} concentration of peptide sequence) and MgHA-APTES-CFP100 (100 μmol·L^{-1} concentration of peptide sequence) were washed with PBS for 10 min and further dried by vacuum at 37 °C for 24 h. The quantity of peptides bound onto the MgHA-APTES surface was assessed as a difference, by measuring the presence of organic functionalities in the washing solutions using NMR spectroscopy.

2.4. *Preliminary* in vitro *tests*

MSCs from mice (C57BL/6 mMSC, Gibco) were cultured in Dulbecco's Modified Eagle Medium (DMEM) (Gibco, GlutaMAX supplement), which contains 10% fetal bovine serum (FBS) and 1% penicillin-streptomycin (100 U·mL^{-1} per 100 μg·mL^{-1}). Cells were cultured at 37 °C with 5% CO_2. Tripsinization was used to detach the cells from the culture flask. Detached cells were further centrifuged and re-suspended. The trypan blue dye exclusion test was used to analyze cell number and viability.

Each MgHA-based disk was washed three times with PBS for 10 min each. Air-dried samples were sterilized by UV for 20 min in a laminar flow hood. Individual samples were placed in separate wells in a 24-well plate. The MSCs (5 × 10^3) were seeded into 24-well inserts of 8 μm pore size (polyethylene terephthalate membrane, Corning) in direct contact with the disks.

We prepared 5 mg·mL^{-1} of the reagent 3-(4,5-dimethylthiazol-2-yl)-2,5-diphenyltetrazolium bromide (MTT, Invitrogen) in 1 × PBS. After 3 days of culture, inserts were moved to a new plate and incubated in 500 μg·mL^{-1} MTT at 37 °C for 2 h. The medium was collected and the cells were incubated with 1 mL of dimethyl sulfoxide for 15 min. In the MTT reagent, metabolically active cells and tetrazolium salt react to produce a formazan dye. The absorbance that was measured at a λ_{max} of 570 nm with a Multiskan FC Microplate Photometer (Thermo Scientific) is correlated with the number of metabolically active cells [20].

3. Results and discussion

3.1. Synthesis of MgHA-APTES disks

The strategy for the immobilization of the chemotactic/haptotactic factors for MSC homing onto the Mg-doped HA disks involved the grafting of APTES in dry hexane. Surface functionalization with APTES, which occurs through a coupling reaction between surface OH groups and silanols obtained from hydrolyzed APTES, allowed the insertion of the amino groups that were required for the immobilization of the peptides used in this study (Fig. 1).

The quantity of amino groups inserted after the silanization process was evaluated by spectrophotometric quantification after a reaction with ninhydrin (Kaiser test). The NH_2 loading, which was evaluated after washing with hexane and drying the disks, was found to be 0.11 mmol·g^{-1}. An XRD analysis was performed directly on the MgHA and MgHA-APTES disks. As shown in Fig. 2, the crystallinity of the MgHA samples was confirmed by the characteristic diffraction peaks that appeared for both samples at 26°, 30°–34°, 40°, and 46°–53° (2θ), which correspond to the (002), (211), (112), (300), (202), (310), (222), (213), and (004) reflection planes of the hydroxyapatite crystal (PDF 09-0432).

The surface morphology of the MgHA-based samples was characterized using SEM and TEM; no significant morphological changes occurred on the Mg-doped HA following the chemical treatments for the surface silanization process (Figs. 3 and 4).

3.2. Conjugation of MgHA-APTES disks with MSCs homing factors

Immobilization of the cell homing factors, FF III$_1$-C or the Gly-Arg-Gly-Asp-Ser-Pro-Lys peptide sequence, onto the Mg-doped HA disks was achieved by classical coupling reactions between the amino groups exposed to the disk surface and the carboxylic

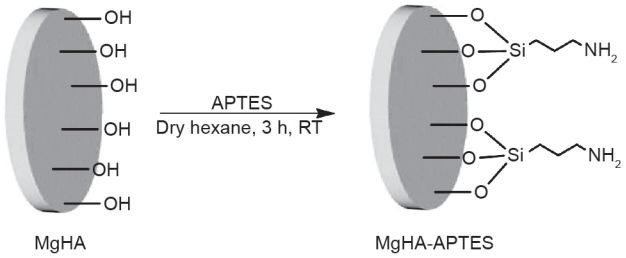

Fig. 1. Scheme of the synthesis of MgHA-APTES disks. RT: room temperature.

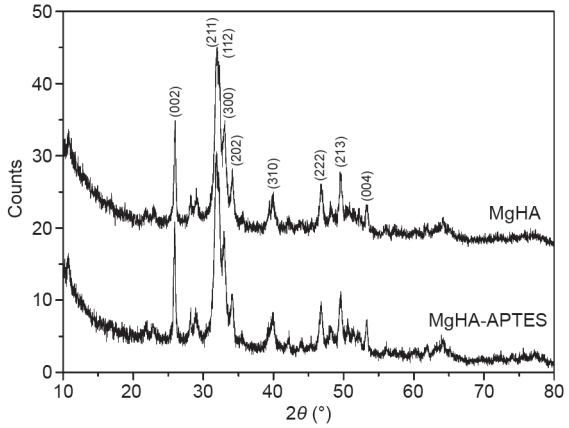

Fig. 2. XRD spectra of MgHA and MgHA-APTES disks.

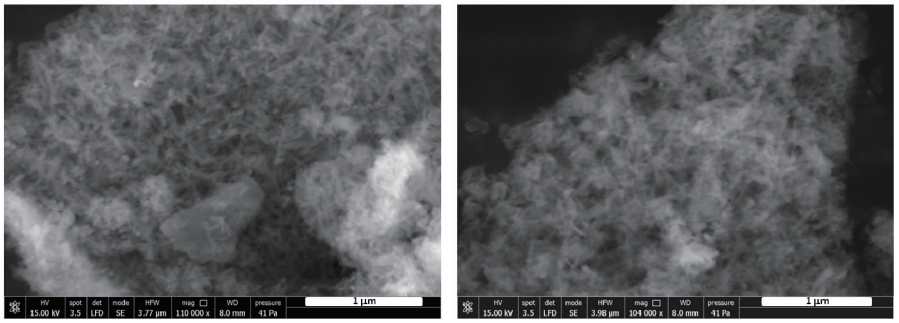

Fig. 3. SEM images of (a) MgHA and (b) MgHA-APTES samples.

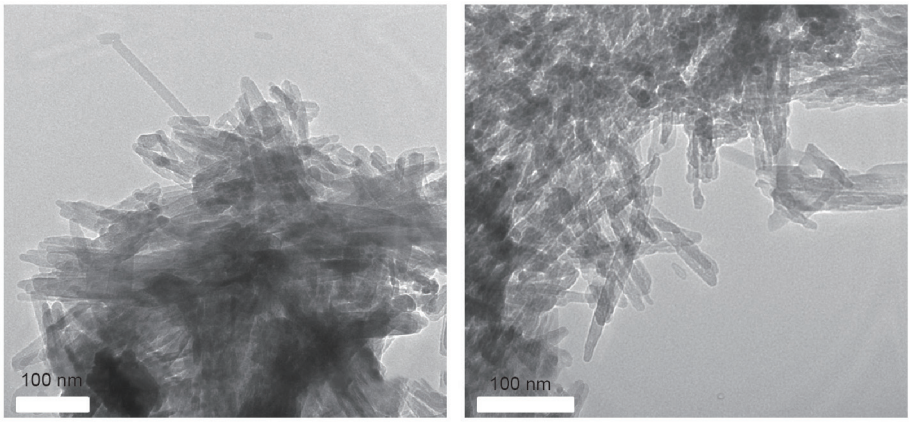

Fig. 4. TEM images of (a) MgHA and (b) MgHA-APTES samples.

functionalities from the peptide sequence, activated when EDC/NHS were used as coupling reagents (Fig. 5). To test the effect of the concentration of cell homing factors on the cell homing behavior, both the FF III_1-C and the peptide sequence were loaded at the two different concentrations of 10 μmol·L^{-1} or 100 μmol·L^{-1}, thus affording two peptide-conjugated samples, MgHA-APTES-CFP10 and MgHA-APTES-CFP100, and two FN-conjugated samples, MgHA-APTES-CFF10 and MgHA-APTES-CFF100.

To determine functionalization reaction effectiveness, TGA was used to confirm the presence of an additional organic moiety on the functionalized material. Fig. 6 shows the distinct shapes of TGA that are related to MgHA, MgHA-APTES, MgHA-APTES-CFP100, and MgHA-APTES-CFF100. The degree of functionalization for each sample, shown as percentage of weight loss at 500 °C under inert atmosphere, reveals the increase of organic mass on the MgHA disk surfaces. A 5% weight loss was observed for MgHA-APTES, as compared with the precursor MgHA sample, while higher weight losses were observed for the peptide- and FN-conjugated samples (8% for MgHA-APTES-CFP100 and 10% for MgHA-APTES-CFF100).

To further characterize the covalent biofunctionalization of the MgHA disks with the peptide sequences, FTIR analyses were performed. Fig. 7 reports the FTIR spectra of unfunctionalized MgHA, MgHA-APTES, and MgHA-APTES-CFF100 samples. All the spectra show absorption peaks at 556 cm^{-1}, 596 cm^{-1}, and 1017 cm^{-1} of the phosphate matrix. In the MgHA-APTES sample, the presence of additional new bands at 2930 cm^{-1} (from the CH_2 stretching) and at 1560 cm^{-1} and 1460 cm^{-1} (due to the N—H bending of the primary aliphatic amine) can be observed. For the MgHA-APTES-CFF100 sample, an additional peak at 1640 cm^{-1} (due to the C=O vibration) is observed. In addition, the peak at 3440 cm^{-1} may ascribe to the O—H vibration and the N—H stretching of the functional groups present on the peptide moieties.

3.3. *Preliminary* in vitro *biological evaluation*

A preliminary biological evaluation of mMSC viability, 3 days after seeding, was analyzed by an MTT test (Fig. 8). The quantification of metabolically active cells, which were seeded into the inserts and placed in direct contact with the MgHA-CFP and MgHA-CFF disks, showed a decrease in stem cell number compared with the non-functionalized MgHA disk and the cells-only group; thus, the results suggested that cells migrated through the insert to the disks in response to the grafted cell homing motifs.

This study offers a platform that is based on the well-known osteoconductive MgHA, combined with tethered cell homing stimuli. It is commonly known that, in certain pathologies and particularly those related to aging (e.g., osteoporotic sites), the number of endogenous MSCs drastically decreases. Therefore, it is necessary to attract MSCs to the specific anatomic sites where they are strongly needed. Current pharmacological treatments, whether alone or combined with biomaterials (e.g., cements, granules, and 3D scaffolds), fail to restore patients' mobility and quality of life, at expensive social costs. The proposed approach shows the possibility of grafting specific motifs involved in MSCs homing onto MgHA. The resulting functionalized biomaterials represent the building blocks for complex treatments through which it will be simultaneously possible to enhance endogenous

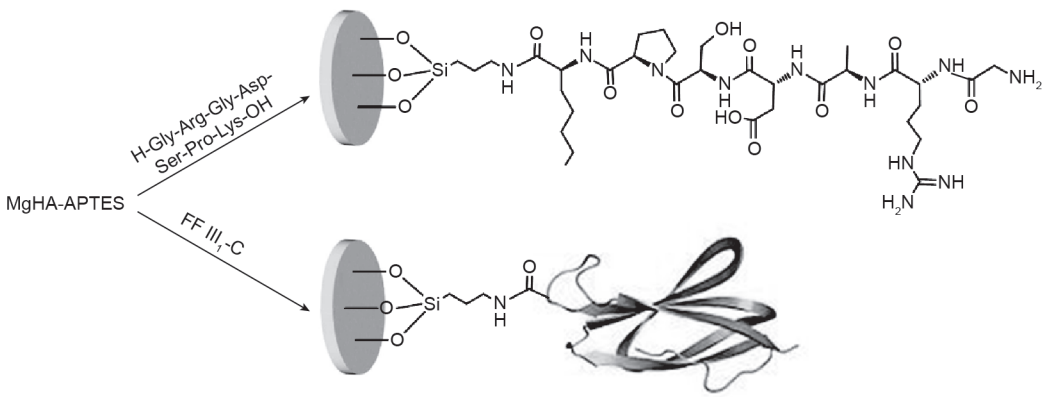

Fig. 5. Scheme of the synthesis of MgHA-APTES-CFP and MgHA-APTES-CFF. Reagents and conditions: Gly-Arg-Gly-Asp-Ser-Pro-Lys or FF III_1-C, EDC·HCl, NHS, PBS, 3 h, 37 °C.

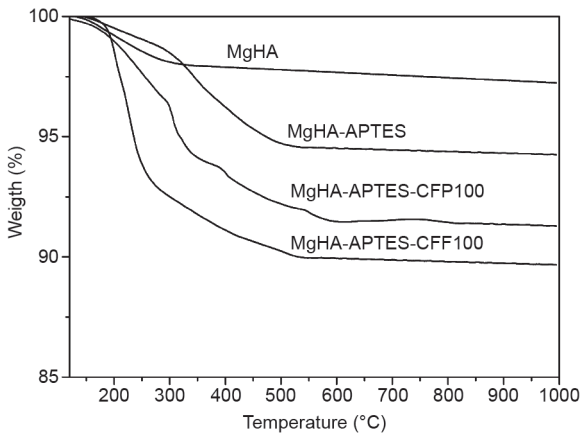

Fig. 6. TGA profiles of MgHA, MgHA-APTES, MgHA-APTES-CFP100, and MgHA-APTES-CFF100 samples.

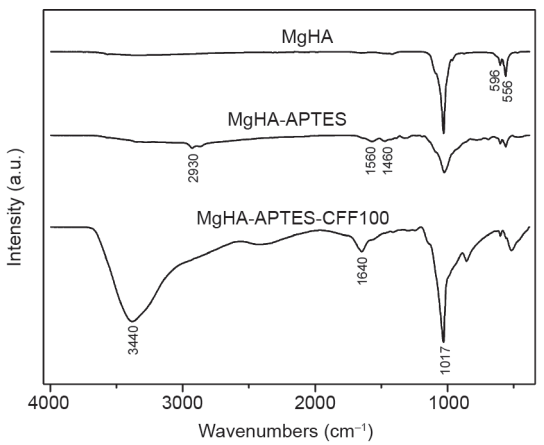

Fig. 7. FTIR spectra of MgHA, MgHA-APTES, and MgHA-APTES-CFF100.

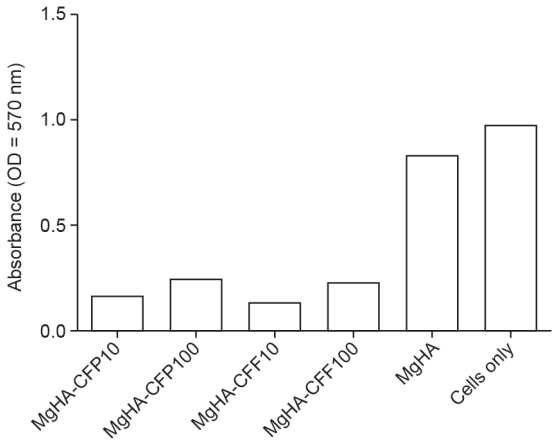

Fig. 8. MTT test of mMSC, 3 days after the seeding into the inserts placed in direct contact with the disks. Cells-only group used as a control.

MSC migration and provide a suitable substrate/environment for MSC adhesion, proliferation, and differentiation in specific bone cells (i.e., osteoblasts).

4. Conclusions

In order to explore whether the incorporation of mimetic peptide sequences on Mg-doped HA may regulate MSC homing, we have reported the grafting of MgHA disks with two chemotactic/haptotactic factors: either FF III_1-C, or the Gly-Arg-Gly-Asp-Ser-Pro-Lys peptide sequence, which is an FN analog that is able to bind to integrin. The cell homing factors, at concentrations of 10 μmol·L^{-1} or 100 μmol·L^{-1}, were covalently linked to the disk surface by means of the APTES linker. Preliminary biological evaluation of mMSC viability, analyzed by MTT test, suggested that the stem cells migrated through the insert to the MgHA disks in response to the grafted cell homing stimuli. Although a deepened understanding of the complex pathways of biomolecules involved in MSC homing is necessary, this preliminary study opens up new opportunities to achieve effective therapeutic outcomes for bone tissue regeneration that can be translated into the clinic.

Compliance with ethics guidelines

Alessandro Pistone, Daniela Iannazzo, Claudia Espro, Signorino Galvagno, Anna Tampieri, Monica Montesi, Silvia Panseri, and Monica Sandri declare that they have no conflict of interest or financial conflicts to disclose.

References

[1] Laurencin CT, Khan Y. Regenerative Engineering. Sci Transl Med 2012; 4(160):160ed9.
[2] Amini AR, Laurencin CT, Nukavarapu SP. Bone tissue engineering: recent advances and challenges. Crit Rev Biomed Eng 2012;40(5):363–408.
[3] Dawson JI, Kanczler J, Tare R, Kassem M, Oreffo RO. Concise review: bridging the gap: bone regeneration using skeletal stem cell-based strategies—where are we now? Stem Cells 2014;32(1):35–44.
[4] Wang P, Zhao L, Liu J, Weir MD, Zhou X, Xu HH. Bone tissue engineering via nanostructured calcium phosphate biomaterials and stem cells. Bone Res 2014;2:14017.
[5] Gong T, Xie J, Liao J, Zhang T, Lin S, Lin Y. Nanomaterials and bone regeneration. Bone Res 2015;3:15029.
[6] Iannazzo D, Pistone A, Espro C, Galvagno S. Drug delivery strategies for bone tissue regeneration. In: Panseri S, Taraballi F, Cunha C, editors Biomimetic approaches for tissue healing. Foster City: OMICS Group eBooks; 2015. p. 1–39.
[7] Panseri S, Cunha C, D'Alessandro T, Sandri M, Russo A, Giavaresi G, et al. Magnetic hydroxyapatite bone substitutes to enhance tissue regeneration: evaluation *in vitro* using osteoblast-like cells and *in vivo* in a bone defect. PLoS One 2012;7(6):e38710.
[8] Cunha C, Panseri S, Iannazzo D, Piperno A, Pistone A, Fazio M, et al. Hybrid composites made of multiwalled carbon nanotubes functionalized with Fe_3O_4 nanoparticles for tissue engineering applications. Nanotechnology 2012;23(46):465102.
[9] Wang DX, He Y, Bi L, Qu ZH, Zou JW, Pan Z, et al. Enhancing the bioactivity of Poly(lactic-*co*-glycolic acid) scaffold with a nano-hydroxyapatite coating for the treatment of segmental bone defect in a rabbit model. Int J Nanomedicine 2013;8:1855–65.
[10] Yoshikawa H, Myoui A. Bone tissue engineering with porous hydroxyapatite ceramics. J Artif Organs 2005;8(3):131–6.
[11] Bellucci D, Sola A, Gazzarri M, Chiellini F, Cannillo V. A new hydroxyapatite-based biocomposite for bone replacement. Mater Sci Eng C Mater Biol Appl 2013;33(3):1091–101.
[12] Pistone A, Iannazzo D, Panseri S, Montesi M, Tampieri A, Galvagno S. Hydroxyapatite-magnetite-MWCNT nanocomposite as a biocompatible multifunctional drug delivery system for bone tissue engineering. Nanotechnology 2014;25(42):425701.
[13] Laurencin D, Almora-Barrios N, de Leeuw NH, Gervais C, Bonhomme C, Mauri F, et al. Magnesium incorporation into hydroxyapatite. Biomaterials 2011;32(7):1826–37.
[14] Landi E, Logroscino G, Proietti L, Tampieri A, Sandri M, Sprio S. Biomimetic Mg-substituted hydroxyapatite: from synthesis to *in vivo* behaviour. J Mater Sci Mater Med 2008;19(1):239–47.
[15] Barthes J, Özçelik H, Hindié M, Ndreu-Halili A, Hasan A, Vrana NE. Cell microenvironment engineering and monitoring for tissue engineering and regenerative medicine: the recent advances. Biomed Res Int 2014;2014:921905.
[16] Schantz JT, Chim H, Whiteman M. Cell guidance in tissue engineering: SDF-1 mediates site-directed homing of mesenchymal stem cells within three-dimensional polycaprolactone scaffolds. Tissue Eng 2007;13(11):2615–24.
[17] Vo TN, Kasper FK, Mikos AG. Strategies for controlled delivery of growth factors and cells for bone regeneration. Adv Drug Deliv Rev 2012;64(12):1292–309.
[18] García AJ, Reyes CD. Bio-adhesive surfaces to promote osteoblast differentiation and bone formation. J Dent Res 2005;84(5):407–13.
[19] Yun YR, Pham BH, Yoo YR, Lee S, Kim HW, Jang JH. Engineering of self-assembled fibronectin matrix protein and its effects on mesenchymal stem cells. Int J Mol Sci 2015;16(8):19645–56.
[20] Liu Y, Peterson DA, Kimura H, Schubert D. Mechanism of cellular 3-(4,5-dimethylthiazol-2-yl)-2,5-diphenyltetrazolium bromide (MTT) reduction. J Neurochem 1997;69(2):581–93.